VU VRIJE UNIVERSITEIT AMSTERDAM

VU Research Portal

Multi-Sensor Historical Climatology of Satellite-Derived Global Land Surface Moisture

Owe, M.; de Jeu, R.A.M.; Holmes, T.R.H.

published in
Journal of Geophysical Research
2008

DOI (link to publisher)
10.1029/2007JF000769

document version
Publisher's PDF, also known as Version of record

Link to publication in VU Research Portal

citation for published version (APA)
Owe, M., de Jeu, R. A. M., & Holmes, T. R. H. (2008). Multi-Sensor Historical Climatology of Satellite-Derived Global Land Surface Moisture. *Journal of Geophysical Research*, *113*, [F01002]. https://doi.org/10.1029/2007JF000769

General rights
Copyright and moral rights for the publications made accessible in the public portal are retained by the authors and/or other copyright owners and it is a condition of accessing publications that users recognise and abide by the legal requirements associated with these rights.

- Users may download and print one copy of any publication from the public portal for the purpose of private study or research.
- You may not further distribute the material or use it for any profit-making activity or commercial gain
- You may freely distribute the URL identifying the publication in the public portal ?

Take down policy
If you believe that this document breaches copyright please contact us providing details, and we will remove access to the work immediately and investigate your claim.

E-mail address:
vuresearchportal.ub@vu.nl

Download date: 05. May. 2023

Multisensor historical climatology of satellite-derived global land surface moisture

Manfred Owe,[1] Richard de Jeu,[2] and Thomas Holmes[2]

Received 1 February 2007; revised 27 April 2007; accepted 26 September 2007; published 18 January 2008.

[1] A historical climatology of continuous satellite-derived global land surface soil moisture is being developed. The data consist of surface soil moisture retrievals derived from all available historical and active satellite microwave sensors, including Nimbus-7 Scanning Multichannel Microwave Radiometer, Defense Meteorological Satellites Program Special Sensor Microwave Imager, Tropical Rainfall Measuring Mission Microwave Imager, and Aqua Advanced Microwave Scanning Radiometer for EOS, and span the period from November 1978 through the end of 2007. This new data set is a global product and is consistent in its retrieval approach for the entire period of data record. The moisture retrievals are made with a radiative transfer-based land parameter retrieval model. The various sensors have different technical specifications, including primary wavelength, spatial resolution, and temporal frequency of coverage. These sensor specifications and their effect on the data retrievals are discussed. The model is described in detail, and the quality of the data with respect to the different sensors is discussed as well. Examples of the different sensor retrievals illustrating global patterns are presented. Additional validation studies were performed with large-scale observational soil moisture data sets and are also presented. The data will be made available for use by the general science community.

Citation: Owe, M., R. de Jeu, and T. Holmes (2008), Multisensor historical climatology of satellite-derived global land surface moisture, *J. Geophys. Res.*, *113*, F01002, doi:10.1029/2007JF000769.

1. Introduction

[2] Land surface moisture is important in many Earth science disciplines. It is a key link between the land surface and the atmosphere. Soil moisture is an important parameter for many energy balance-related modeling applications, such as numerical weather forecasting, climate prediction, radiative transfer modeling, global change modeling, and other land processes models. Soil moisture usually exhibits a high degree of spatial variability. However, these spatial differences are not always entirely intuitive, and are a function not only of rainfall distributions, but are the result of topography, heterogeneity of soil physical properties, and land cover characteristics as well. Soil moisture is also thought to be the single most important parameter influencing the atmospheric circulation over land during the summer. Improved estimates of spatially representative surface moisture will significantly enhance both short- and long-term precipitation forecasts. The soil surface is the transitional link between the soil water storage and atmospheric moisture. Surface soil moisture influences the partitioning of the incoming energy into latent and sensible heat components. Soil moisture, thus provides a key link between the water and energy balances. Soil moisture was recognized as a parameter of considerable importance by the U.S. Global Change Research Program for improving the accuracy of large-scale land surface-atmosphere interaction models [*National Research Council*, 1990]. Additionally, soil moisture has been identified throughout the new Decadal Survey, and may be the single most important parameter linking the key components of hydrological, biological, and geochemical processes [*National Research Council*, 2007].

[3] From a historical perspective, researchers have had limited information about the large-scale distribution of soil moisture in time and space, since soil moisture is not routinely acquired like many hydrometeorological measurements. Consequently, long-term observational data at the global scale, do not exist. While isolated observational data sets are available [*Robock et al.*, 2000; *Brock et al.*, 1995; *Hollinger and Isard*, 1994], they are largely regional in nature, and rarely extend beyond several years duration. Furthermore, while in situ observations are generally accurate, they still are point measures, and are not always readily transformed into spatial averages, especially at regional, continental, and global scales.

[4] Space-based remote sensing offers potentially the greatest single contribution to large-scale monitoring of the Earth's surface. If properly utilized, satellite systems can offer the spatial, temporal, and spectral resolution necessary for consistent and continuous uninterrupted coverage of the whole Earth environment and its surrounding

[1]Hydrological Sciences Branch, NASA Goddard Space Flight Center, Greenbelt, Maryland, USA.
[2]Department of Geo-Environmental Sciences, Vrije Universiteit Amsterdam, Amsterdam, Netherlands.

This paper is not subject to U.S. copyright.
Published in 2008 by the American Geophysical Union.

atmosphere. Such detailed observations are necessary in order to detect often subtle environmental changes. Remote sensing technology is central to the integration of many interrelated but highly variable point-scale phenomena to more useful, regionally oriented land surface processes.

[5] A historical data set of global surface soil moisture is being developed from satellite microwave brightness temperature observations. The data are derived from several different satellite sensors beginning in late 1978 and will continue to the end of 2007. The surface moisture retrievals are made with a Land Parameter Retrieval Model (LPRM), developed by researchers from the NASA Goddard Space Flight Center (GSFC) and the Vrije Universiteit Amsterdam (VU) [*Owe et al.*, 2001]. Because the data are derived from several sensors with different radiometric characteristics, some differences in sensing depth, spatial resolution, and orbit characteristics do exist. However, specifications for all sensors are well documented in the literature, and a complete list of references is provided with the data. The data are expected to be available for download in mid-2008, from the Goddard Earth Sciences Data and Information Services Center (GES DISC) and the Vrije Universiteit Amsterdam, Netherlands. These data sets should prove valuable for many environmental modeling and monitoring applications.

2. General Background

2.1. Soil Moisture Modeling and Retrieval

[6] A variety of modeling techniques have been developed to estimate soil moisture from microwave brightness temperature observations. Results from early field and aircraft experiments demonstrated strong regression-based relationships between surface moisture and both brightness temperature and surface emissivity [*Schmugge*, 1976, 1977; *Jackson et al.*, 1984]. Models have subsequently become more complex by accounting for canopy effects [*Mo et al.*, 1982; *Jackson et al.*, 1982; *Jackson and Schmugge*, 1991], roughness [*Choudhury et al.*, 1979], polarization mixing [*Wang and Choudhury*, 1981], and other perturbing factors [*Jackson and O'Neill*, 1987; *Jackson et al.*, 1992, 1997; *O'Neill and Jackson*, 1990]. While many of these models are based on radiative transfer theory, an element of empiricism often remains because of difficulty in parameterizing some components from other measurable biophysical properties and at more meaningful spatial scales.

[7] Studies have shown good agreement between soil moisture derived from microwave-based models and field observations [*Owe et al.*, 1992; *Jackson*, 1997; *Drusch et al.*, 2001; *Jackson and Hsu*, 2001]. However, an inherent problem with ground measurements has been the issue of scaling point observations to sensor footprint-sized averages, especially at satellite scales. This task becomes increasingly problematic with increasing land cover heterogeneity. The lack of large-scale surface moisture observations, has often forced researchers to calculate soil wetness indices (e.g., Antecedent Precipitation Index) from more readily available meteorological data, for comparison to satellite observations [*McFarland*, 1976; *Wilke and McFarland*, 1986; *Owe et al.*, 1988, *Ahmed*, 1995; *Achutuni and Schofield*, 1997]. *McFarland and Neale* [1991] developed a regression technique that used brightness temperatures from several Special Sensor Microwave Imager (SSM/I) channels in a series of three empirical equations that accounted for different vegetation density classes. However, this approach calculated a soil wetness index, and was calibrated to regional Antecedent Precipitation Index calculations for test sites in the U.S. Southern Great Plains region. Errors associated with this method were found to be quite high, and its application to other locations and at global scales may therefore be less useful, especially in data-poor regions where validation and recalibration may be more difficult. These approaches have successfully demonstrated the spatial and temporal sensitivity of satellite sensors, and have also been extremely useful for studying long-term seasonal and interannual climatologies. However, wetness indices do not necessarily relate directly to actual surface moisture quantities, and therefore their value is limited for use in many environmental monitoring and modeling applications.

[8] Only a few modeling approaches can be considered true retrieval. These techniques are, for the most part, physically based and account for most of the major components in radiative transfer theory. They typically solve for the soil emissivity, from which volumetric soil moisture is subsequently derived by inverting the Fresnel relationships and a dielectric mixing model [*Schmugge*, 1985]. The model developed by *Jackson* [1993] has compared well with aircraft data from several large field experiments [*Jackson et al.*, 1995, 1999]. The model has also performed well with Tropical Rainfall Measuring Mission (TRMM) Microwave Imager (TMI) and SSM/I measurements over these same experimental sites [*Jackson and Hsu*, 2001; *Jackson et al.*, 2002]. However, this approach requires a parameterization of the vegetation water content (VWC) in order to calculate the canopy optical depth [*Jackson et al.*, 1982; *Jackson and Schmugge*, 1991]. While extensive biophysical measurements were made during field experiments from which VWC was calculated, it may be more difficult to obtain this information on a regular basis for application at the global scale.

[9] The method developed by *Njoku and Li* [1999] and *Njoku et al.* [2003] is the official Advanced Microwave Scanning Radiometer (AMSR-E) soil moisture science team contribution [*Njoku*, 2004]. This approach is based on polarization ratios, which effectively eliminate or minimize the effects of surface temperature. The original approach used six microwave channels (three frequencies, each at two polarizations) to solve for three land surface parameters (soil moisture, vegetation water content, and surface temperature). It was expected to provide surface soil moisture with an accuracy of 6% absolute moisture content (0.06 cm^3 cm^{-3}) in areas with low vegetation biomass (< 1.5 kg m^{-2}). However, unanticipated radio frequency interference (RFI) problems were encountered at the 6.9 GHz frequency, requiring modification of this approach [see *Njoku*, 2004].

[10] Another recently developed retrieval approach is based on the microwave polarization difference index [*Owe et al.*, 2001; *De Jeu and Owe*, 2003; *Meesters et al.*, 2005]. This method uses a forward modeling optimization procedure to solve a radiative transfer equation for both soil moisture and vegetation optical depth, and requires no calibration or fitting parameters, or other biophysical meas-

Table 1. Specifications for the Various Microwave Sensors Used in Deriving the Soil Moisture Data Sets[a]

Parameter	SMMR	SSM/I	TMI	AMSR-E
Frequencies, GHz	6.6, 10.7, 18, 37	19.3, 36.5	10.7, 19.4, 37	6.9, 10.7, 18.7, 36.5
Polarization	H,V all frequation	H,V all frequation	H,V all frequation	H,V all frequation
Incidence angle	50.2°	53.1°	52.88°	55°
Swath width, km	780	1394	759	1445
Orbit type	polar	polar	N38° to S38°	polar
		Equator Crossing		
Ascending orbit	1200 LST	see Table 3	variable	1330
Descending orbit	2400 LST	see Table 3	variable	0130
Data period	Nov 1978 to Aug 1987	Jul 1987 to present	Dec 1997 to present	May 2002 to present

[a]Abbreviations are as follows: AMSR-E, Advanced Microwave Scanning Radiometer for EOS; SSM/I, Special Sensor Microwave/Imager; SMMR, Scanning Multichannel Microwave Radiometer; TMI, Tropical Rainfall Measuring Mission Microwave Imager.

urements during the retrieval process. A unique feature of this approach is that it may be applied at any relevant microwave frequency, and it was used in the retrieval of the data sets described in this paper. A more detailed description of this model is provided in section 4.

2.2. Sensors and Specifications

[11] The soil moisture data sets were derived from measurements obtained from a variety of satellite sensors beginning in late 1978. All sensors have several common wave bands, while some wave bands are either unique or common to only two or three of the satellite systems. Comparative specifications for the different sensors are provided in Tables 1 and 2. Brief descriptions of the four sensors are provided, however, readers are referred to the various references provided for a more comprehensive discussion.

[12] The Scanning Multichannel Microwave Radiometer (SMMR) was flown onboard the Nimbus-7 satellite [*Gloersen and Barath*, 1977; *Gloersen et al.*, 1984]. The instrument was launched in October 1978 and was eventually deactivated in August 1987. Power constraints onboard the Nimbus satellite permitted data acquisition on alternate days only, however, the 24 hour on-off cycle still permitted both day and night observations. The satellite orbited the Earth approximately 14 times per day, with a local solar noon and midnight equator crossing. Because of the on-off instrument cycling, complete global coverage required 6 days. SMMR brightness temperatures were measured at five frequencies, from 6.6 GHz to 37 GHz, at both horizontal and vertical polarization. Spatial resolution of SMMR was comparatively coarse, relative to later instruments (from approximately 25 km at 37 GHz to almost 150 km at 6.6 GHz) [*National Snow and Ice Data Center* (*NSIDC*), 2005a].

[13] The Special Sensor Microwave Imager (SSM/I) is found on board a series of Defense Meteorological Satellite Program (DMSP) platforms designated F-8, F-10, F-11, F-13, F-14, F-15, and F-16. The first satellite was launched in July 1987, while the last one was launched in October 2003. Orbit characteristics are very similar to Nimbus-7 (see Table 1). Equator crossing times vary between the different satellites and are provided in Table 3 [*Armstrong et al.*, 1994; *NSIDC*, 2005b].

[14] Tropical Rainfall Measuring Mission (TRMM) Microwave Imager (TMI) began acquiring data in December 1997. The TMI instrument is a nine channel radiometer, based largely on SSM/I technology. However, unlike the previous platforms, TRMM is in a near-equatorial orbit, so as to maximize observations over tropical ocean regions. Orbit characteristics are less straightforward than polar orbiting platforms. The satellite orbit is in a constant plane relative to the sun, with about 16 orbits per day. The Earth's inclination and rotation, therefore, results in a sine wave-like pattern of Earth coverage between about 38° north and south latitude, with local overpass times drifting over the entire 24-hour day approximately once each month [*Kummerow et al.*, 1998] (see also http://tsdis.gsfc.nasa.gov/).

[15] The Advanced Microwave Scanning Radiometer (AMSR-E) on the AQUA Earth observation satellite was launched in May 2002. The sensor is 12 channels (six frequencies), with 4 bands relevant to soil moisture retrieval. Orbit characteristics are somewhat similar to its predecessor, SMMR, although the AMSR-E swath width is nearly twice as wide at 1445 km. Daily Earth coverage is nearly 100% above and below 45° north and south latitude, while midlatitudes

Table 2. Footprint Dimensions Corresponding to the Different Sensors at all Wavelengths Relevant to Soil Moisture Retrieval[a]

	Footprint Size, km–GHz			
	6.x	10.7	18–19	36–37
SMMR	148 × 95	91 × 59	55 × 41	27 × 18
SSM/I	na[b]	na	69 × 43	37 × 28
TMI	na	63 × 39	30 × 18	16 × 10
AMSR-E	74 × 43	51 × 30	27 × 16	14 × 8

[a]Dimensions are along track × cross track. Abbreviations are as follows: AMSR-E, Advanced Microwave Scanning Radiometer for EOS; na, not applicable; SSM/I, Special Sensor Microwave/Imager; SMMR, Scanning Multichannel Microwave Radiometer; TMI, Tropical Rainfall Measuring Mission Microwave Imager.
[b]Na means not applicable.

Table 3. Equator Crossing Times for the Defense Meteorological Satellite Program Satellite Platforms[a]

	Equator Crossing Times, LST	
SSM/I Platform	Ascending Orbit	Descending Orbit
F-8	1812	0612
F-11	1710	0510
F-13	1735	0535
F-14	2021	0821
F-15	2131	0931
F-16	2013	0813

[a]SSM/I, Special Sensor Microwave/Imager.

experience about 80% coverage [*Ashcroft and Wentz*, 2003; *NSIDC*, 2006].

2.3. Original Data Archives

[16] All sensor data were downloaded as brightness temperatures from their public source archives. SMMR, SSM/I, and AMSR-E data are available from the National Snow and Ice Data Center (NSIDC) in Boulder Colorado (http://nsidc.org/). However, SSM/I brightness temperature data products are only available for the F-8, F-11, and F-13 satellites from *NSIDC* [2005b]. TMI data were downloaded from the Goddard Earth Sciences Data and Information Services Center (GES DISC), formerly known as the Goddard Distributed Active Archive Center (DAAC) (http://disc.sci.gsfc.nasa.gov/index.shtml).

3. Theoretical Background

[17] Radiometric temperature readings in the microwave region have been shown to yield important information on moisture phenomena in the environment, including surface soil moisture. Microwave remote sensing is the only technology that provides a direct measure of the absolute moisture contained in the environment. Thermal radiation in the microwave region is emitted by all natural surfaces, and is a function of both the land surface and the atmosphere. The brightness temperature (T_{Bp}) observed by a satellite sensor is a function of the land surface emission as well a contribution from the atmosphere, such that

$$T_{Bp} = T_u + \exp(-\tau_a)\left[T_{bp} + r_p T_d\right] \quad (1)$$

Where T_u and T_d are the upwelling and downwelling atmospheric emissions respectively, τ_a is the atmospheric opacity, r_p is the surface reflectivity, and T_{bp} is the surface brightness temperature. The subscript p denotes either horizontal (H) or vertical (V) polarization. The surface brightness temperature is a function of the physical temperature of the radiating body and its emissivity, according to

$$T_{bp} \cong e_{sp} T_s \quad (2)$$

where T_s is the thermodynamic temperature of the emitting layer, and e_{sp} is the smooth-surface emissivity. The emissivity may be further defined as

$$e_{sp} = \left(1 - R_{sp}\right) \quad (3)$$

where R_s is the smooth-surface reflectivity. The absolute magnitude of the soil emissivity is lower at H polarization than at V polarization. However, the sensitivity to changes in soil moisture is considerably greater at H polarization than at V polarization. Conversely, at V polarization, the sensitivity to surface temperature is greater. This phenomenon forms the basis for surface temperature retrieval techniques by microwave radiometry [*Owe and Van de Griend*, 2001].

[18] Soil emissivity is a function of its dielectric properties. The dielectric constant is defined as a complex number, where the real part determines the propagation characteristics of the energy as it passes upward through the soil, and the imaginary part determines the energy losses. In a heterogeneous medium such as soil, the complex dielectric constant is a combination of the individual dielectric constants of its constituent parts, and includes air, water, rock, etc. Other factors which will influence the dielectric constant include temperature, salinity, soil texture, and wavelength. The dielectric constant is a difficult quantity to measure on a routine basis outside the laboratory, and values are generally derived from dielectric mixing models [*Dobson et al.*, 1985; *Wang and Schmugge*, 1980].

[19] Microwave energy originates from within the soil, and the contribution of any one soil layer decreases with depth. For practical purposes, the surface layer provides most of the measurable energy contribution and is defined as the thermal sampling depth [*Schmugge*, 1983], although it is also commonly referred to as the skin depth or observation depth. The thickness of this layer is thought to be only several tenths of a wavelength thick. However, its actual thickness will vary according to moisture content, wavelength, polarization, and incidence angle. As the average moisture content of this layer decreases, its thickness increases. It is the average dielectric properties of this layer that determines the observed emissivity. Soil moisture retrieval from microwave measurements is made possible owing to the large contrast between the dielectric constants of dry soil ($\sim$4) and water ($\sim$80). This contrast results in a wide range in the dielectric properties of soil-water mixtures (from about 4 to about 40), and is the primary influence on the natural microwave emission from the soil [*Schmugge*, 1985].

[20] Increasing incidence angle will decrease the soil emission at horizontal polarization. Furthermore, a greater viewing angle also increase the path length of the upwelling radiation, making it more susceptible to attenuation effects of the atmosphere and vegetation canopies.

[21] Vegetation affects the microwave emission as observed from above the canopy in two ways. First, vegetation will absorb or scatter the radiation emanating from the soil. Secondly, the vegetation will also emit its own radiation. These two effects tend to counteract each other. The observable soil emission will decrease with increased vegetation, while emission from the vegetation will increase. Under a sufficiently dense canopy, the emitted soil radiation will become totally masked, and the observed emissivity will be due largely to the vegetation. The magnitude of the absorption depends upon the wavelength and the water content of the vegetation. The most frequently used wavelengths for soil moisture sensing are in the L and C bandwidths ($\sim$1.4 and $\sim$6 GHz respectively), with L-band sensors having greater penetration of vegetation. While observations at all frequencies are subject to scattering and absorption and require some correction if the data are to be used for soil moisture retrieval, shorter wave bands are more susceptible to vegetation influences. A variety of models have been developed to account for the effects of vegetation on the observed microwave signal, and range from empirical linear models [*Jackson et al.*, 1982; *Ahmed*, 1995; *Owe et al.*, 1988], to more physically based radiative transfer treatments [*Mo et al.*, 1982; *Njoku and Li*, 1999; *Wigneron et al.*, 1995; *Wegmuller et al.*, 1995].

[22] The radiation from the land surface as observed from above the canopy may be expressed in terms of the radiative brightness temperature, T_{bp}, and is given as a simple radiative transfer equation [*Mo et al.*, 1982],

$$T_{bp} = T_S e_{rp} \Gamma_p + (1 - \omega_p) T_C (1 - \Gamma_p) + (1 - e_{rp})(1 - \omega_p) Tc (1 - \Gamma_p) \Gamma_p \quad (4)$$

where T_S and T_C are the thermodynamic temperatures of the soil and the canopy respectively, ω is the single scattering albedo, and Γ is the transmissivity. The first term of the above equation defines the radiation from the soil as attenuated by the overlying vegetation. The second term accounts for the upward radiation directly from the vegetation, while the third term defines the downward radiation from the vegetation, reflected upward by the soil and again attenuated by the canopy. The transmissivity is further defined in terms of the optical depth, τ, and incidence angle, u, such that

$$\Gamma = \exp(-\tau / \cos u) \quad (5)$$

The optical depth is strongly related to the canopy density, and for frequencies less than 10 GHz, it can be expressed as a linear function of vegetation water content [*Jackson et al.*, 1982]. Maximum values for τ were found to be about 1.3 at C band for a soybean canopy with a vegetation water content of about 1.5 kg m^{-2} [*Mo et al.*, 1982]. However, the same canopy yields an optical depth of only 0.35 at L band. An optical depth of 1.3 translates to a transmissivity of about 0.13, which indicates minimal penetration of the soil signal through the canopy at C band. Furthermore, it was shown that at C band, the above-canopy signal becomes totally saturated at an optical depth of about 1.5 ($\omega = 0.06$) in the horizontal channel, although for practical purposes, the sensitivity is already quite low above 0.75 [*Owe et al.*, 2001]. At low soil moisture conditions, this threshold is seen to occur even sooner. In another study, African savannas were found to exhibit an annual course for the optical depth that varied from about 0.4 to 0.7 [*Van de Griend and Owe*, 1994].

[23] The single scattering albedo describes the scattering of the soil emissivity by the vegetation, and is a function of plant geometry. The scattering albedo may be calculated theoretically [*Wegmulller et al.*, 1995], however, experimental data for this parameter are limited, and values for selected crops were found to vary from 0.04 to about 0.13 [*Mo et al.*, 1982; *Owe et al.*, 2001]. Few values are found for natural vegetation. A 3-year time series of the scattering albedo at both 6.6 GHz and 37 GHz was calculated for an African savanna region [*Van de Griend and Owe*, 1994]. The scattering albedo exhibited considerable variability during the period, although no relationship with vegetation biomass or other seasonal indicators was observed.

[24] While there is some experimental evidence indicating possible polarization dependence of both the optical depth and the scattering albedo, these differences have been observed mainly during field experiments and over vegetation elements that exhibit some uniform orientation such as vertical stalks in tall grasses, grains, and maize [*Wigneron et al.*, 1995; *Wegmuller et al.*, 1995; *Kirdiashev et al.*, 1979]. However, the canopy and stem structure for most crops and naturally occurring vegetation are randomly oriented. Furthermore, the effects of any systematic orientation exhibited by vegetation elements would most likely be minimized at satellite scales [*Owe et al.*, 2001].

[25] The issue of salinity effects on soil emissions has received only limited attention in the way of field studies and experimental data. *Jackson and O'Neill* [1987] compared modeling results of saline soils using several dielectric mixing models to controlled field measurements with both L- and C-band radiometers. However, observed effects were not found to be as large as the model predictions. The dielectric constant of pure water is approximately 80 at L band (20°C), while only about 73 for sea water (~3.5% saline), with the difference in brightness temperature being only about 5 K. Furthermore, the difference in the dielectric constant between sea water and pure water is considered to be significant only at frequencies below 5 GHz, with only minimal dependence above that frequency [*Rees*, 2001]. Consequently, the salinity effects on soil emissions can be expected to be low at salt concentrations on the order of sea water. However, in regions of high evaporative demand, salt concentrations may be significantly higher, especially from the combined effects of fertilization and irrigation. The resulting effect on the soil emissivity may therefore be greater as well. A priori knowledge of soil salinity conditions could potentially allow investigators to make appropriate adjustments in a dielectric mixing model if the soil dielectric constant were known.

4. Land Parameter Retrieval Model

[26] Polarization ratios, such as the Microwave Polarization Difference Index (MPDI)

$$\mathrm{MPDI} = \left(\mathrm{T_{b(V)}} - \mathrm{T_{b(H)}}\right) / \left(\mathrm{T_{b(V)}} + \mathrm{T_{b(H)}}\right), \quad (6)$$

are frequently used to normalize for temperature dependence, resulting in a parameter that is quantitatively and more highly related to the dielectric properties of the emitting surface(s). At lower frequencies (longer wavelengths), the MPDI will contain information on both the canopy and the soil emission, and consequently the soil dielectric properties as well. The theoretical relationship between the MPDI, vegetation optical depth, and the soil dielectric constant [*Owe et al.*, 2001; *Meesters et al.*, 2005], forms the basis for LPRM optimization. The latter reference describes an analytical solution to this relationship, which improves the accuracy and overall efficiency of the retrieval algorithm, while also allowing one to change the scattering albedo "on the fly."

[27] The retrieval methodology uses a nonlinear iterative procedure in a forward modeling approach to partition the surface emission into its primary source components, i.e., the soil emission and the canopy emission, and then optimizes on the canopy optical depth and the soil dielectric constant. Once convergence between the calculated and observed brightness temperatures is achieved, the model uses a global database of soil physical properties [*Rodell et al.*, 2004] together with a soil dielectric mixing model [*Wang and Schmugge*, 1980] to solve for the surface soil moisture. No field observations of soil moisture, canopy

biophysical properties, or other observations are used for calibration purposes, resulting in a model that is largely physically based with no regional dependence, and is applicable at any microwave frequency suitable for soil moisture monitoring (i.e., L, C, X, or Ku band).

[28] The LPRM does not establish or assume a soil moisture sampling depth during retrieval calculations, nor is there a depth implied by the retrieval, other than in the estimation of an average thermodynamic temperature for the emitting layer, which is assumed to be approximately 3 tenths of the wavelength. It will be left to the individual investigator to make any further assumptions as to the soil moisture sampling depth, based on the sensor used and any additional climate information that one may have available. Land surface temperature is derived directly from 37 GHz vertical polarization brightness temperature observations, in a manner similar to the original model description [*Owe et al.*, 2001, 2005; *O'Neill et al.*, 2006], although additional large-scale field observations and experimental data were used to refine the original relationship. The most reliable emitting layer temperature estimates will occur during the nighttime because of increased thermal equilibrium conditions of the near-surface air, canopy, and surface soil. Daytime emitting layer temperatures are often more difficult to estimate because of more intense surface heating. While this is a significant problem in arid and semiarid locations, it may pose problems in more temperate regions as well, especially in vast agricultural areas, or other locations with a high percentage of exposed soils. However, even though comparisons between daytime and nighttime retrievals have shown good consistency, it is expected that nighttime retrievals will most likely have smaller temperature-related errors than daytime retrievals.

5. Retrieval Data Sets

[29] The LPRM will be used to derive global surface soil moisture for the period November 1978 through December 2007. These data sets will be produced from brightness temperature observations acquired from all available active and historical sensors, including Nimbus-SMMR (1978–1987), DMSP-SSM/I (1987 to present), TRMM-TMI (1997 to present), and AQUA-AMSR-E (2002 to present). In cases where multiple sensors were/are active during the same time period, we will process all available observational data. We will also process multiple frequencies where a given sensor has more than one suitable waveband for soil moisture retrieval. (i.e., SMMR, AMSR-E). All retrieval data sets will be written and stored in Hierarchical Data Format (HDF), which is the accepted standard for all EOS data products. This will ensure maximum compatibility with other EOS-era data sets, and will also ensure maximum compatibility with GES DISC data formatting protocols. Furthermore, HDF retains the Coordinated Universal Time (UTC) time stamp and geo-referencing information of the original orbit data.

[30] Since the soil moisture data are derived from several different satellite sensors with varying spatial resolution and radiometric frequency, investigators should exercise care in the interpretation of these data and when using them in specific applications. The LPRM algorithm has certain known limitations, however, they are due entirely to limitations inherent to microwave theory. Microwave brightness temperatures at X and C band are sensitive to only the soil moisture in the top 1 to 1.5 cm of the soil, averaged over the spatial extent of the footprint. Owing to the masking effects of vegetation on the soil emission, measurements of soil moisture from microwave radiometers are most accurate in areas of low vegetation density. Therefore attenuation of the emission signal from the soil owing to excessive vegetation will usually increase the retrieval error. When the vegetation density is too great, the LPRM will often not achieve convergence. In such cases, pixels are assigned an appropriate nondata flag.

[31] One must consider the radiometric characteristics of the individual sensor in estimating the impact of error sources on the data retrievals. Radiometric frequency is the primary factor influencing a sensor's ability to retrieve soil moisture and determines its effective global coverage. A lower-frequency (longer wavelength) sensor will provide greater coverage for soil moisture retrieval than a sensor of higher frequency, largely owing to its ability to penetrate denser vegetation canopies. It may also be helpful to use other data sets in the interpretation of soil moisture retrievals, for instance terrain and topographic maps, vegetation maps, and land use maps, many of which may be available as digital remote sensing products as well.

[32] Certain other land cover characteristics may also increase the error in data retrievals, and may include excessive surface roughness affecting a significant percentage of the pixel, gross topography such as steep mountainous terrain, significant amount of pixel area occupied by water (as well as coastal pixels), as well as ice snow, and frozen soils. Data screening for snow or frozen surface conditions is limited to flagging those pixels where the surface temperature is observed to be at or below 273 K, as determined by the model's temperature algorithm. All nondata pixels (i.e., water, snow, ice, frozen soils, nonconvergence, etc.) are assigned unique values in order to retain their identity.

[33] It has been determined that RFI may have a significant impact on both H and V polarization brightness temperatures at C band, and to a lesser extent at X band. RFI is usually caused by communications and broadcast signals, and frequently results in abnormally high brightness temperatures. While the existence of RFI has been known for some time, rigorous studies of this phenomenon in Earth observation data (AMSR-E) have only recently been reported [*Li et al.*, 2004; *Njoku et al.*, 2005]. Similar studies should be conducted with other sensors to determine the extent of this problem in historical data as well. The presence of RFI in radiometer data may be identified from original brightness temperature values [*Li et al.*, 2004]. Radio frequency contamination in 6–7 GHz range is seen to be highly prevalent in the U.S., Southwest Asia, and the Middle East, with occurrences in Europe seemingly associated with selected urban locations. RFI in the 10 GHz is less prevalent globally, but appears to be concentrated in several European locations, such as Italy and the United Kingdom [see *Njoku et al.*, 2005]. In the event of extreme RFI, the LPRM will often not achieve convergence. The LPRM will continually test for RFI by calculating the RFI Index as defined by *Li et al.* [2004], and identify such pixels with appropriate data flags.

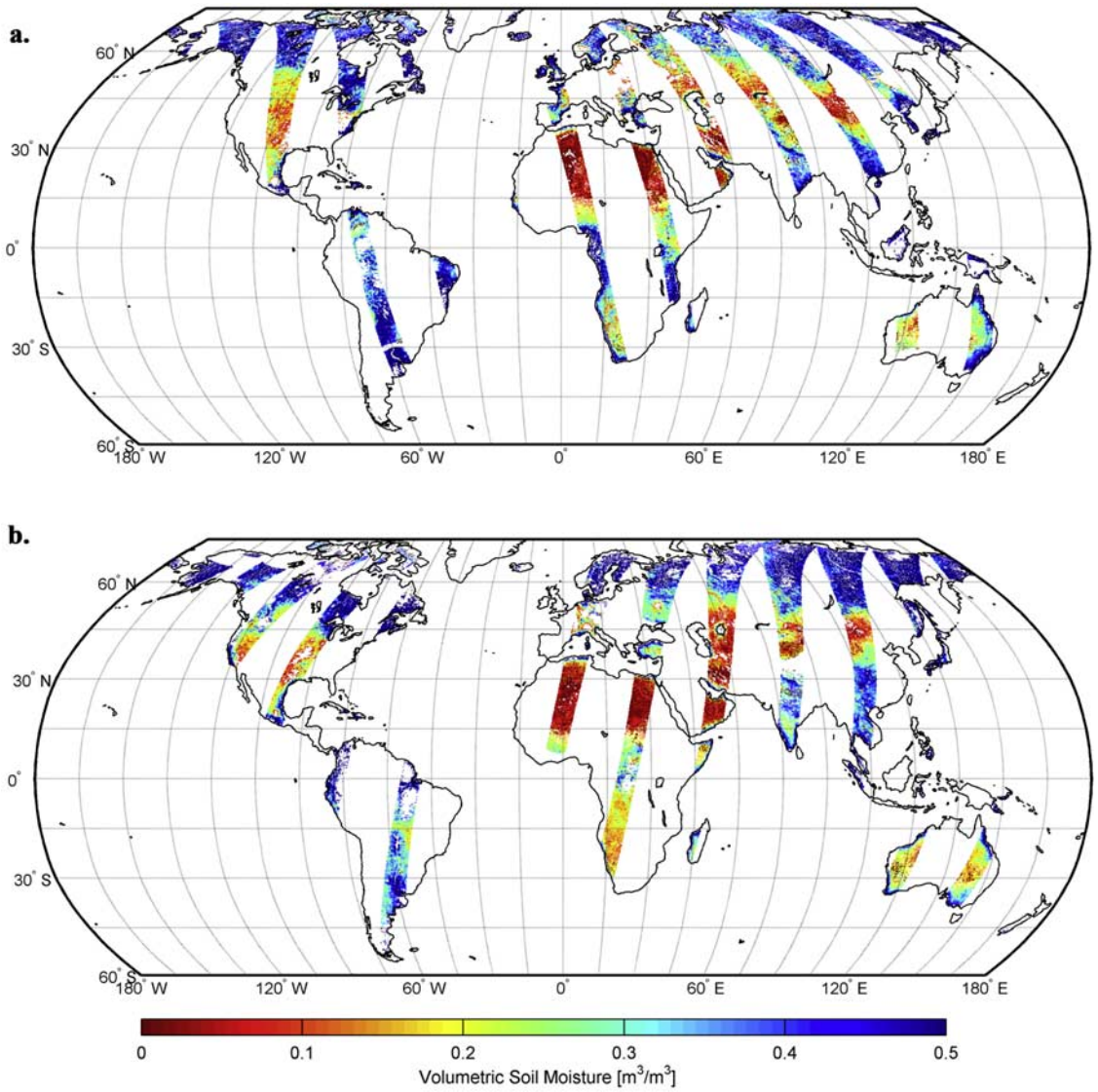

Figure 1. Twenty-four-hour day and night Scanning Multichannel Microwave Radiometer surface soil moisture retrievals for 7 July 1980.

5.1. Scanning Multichannel Microwave Radiometer

[34] SMMR surface moisture retrievals are performed at 6.6, 10.7, and 18 GHz. C band is most susceptible to RFI contamination and has been found to be quite widespread in many global locations for the AMSR-E period (see above). However, its occurrence during the SMMR period has not been fully established, and the availability of the longer-wavelength retrievals for unaffected areas would seem to be highly valuable. As indicated earlier, X-band RFI has been detected in Europe in recent years as well. Consequently, conducting surface moisture retrievals at both bands will maximize global availability of these data. Furthermore, the availability of 18 GHz retrievals will also allow investigators to evaluate the higher-frequency data relative to the contemporaneous longer-wavelength retrievals. Such comparisons will permit improved interpretation of similar higher-frequency surface moisture retrievals from SSM/I measurements during periods when longer-wavelength data are unavailable (for example, during the period after the deactivation of SMMR and the launch of TRMM). Global maps of daytime and nighttime SMMR retrievals are provided, illustrating the extent of daily (24-hour) orbital coverage (Figure 1). Global coverage is achieved in about six days because of the sensor's availability only on alternate days.

[35] Average monthly surface soil moisture maps for the 6.6, 10.7, and 18 GHz bands are also provided for comparison (Figure 2). Both the soil sampling depth and the sensor's ability to penetrate vegetation decreases with frequency, and a subsequent decrease in global coverage of soil moisture is clearly observed as the frequency increases. Since all three frequencies are contained on the same sensor platform, more meaningful direct comparisons between the three wavebands may be possible with these data.

5.2. Special Sensor Microwave Imager

[36] SSM/I retrievals are performed from the end of the SMMR period to the beginning of the AMSR-E period in

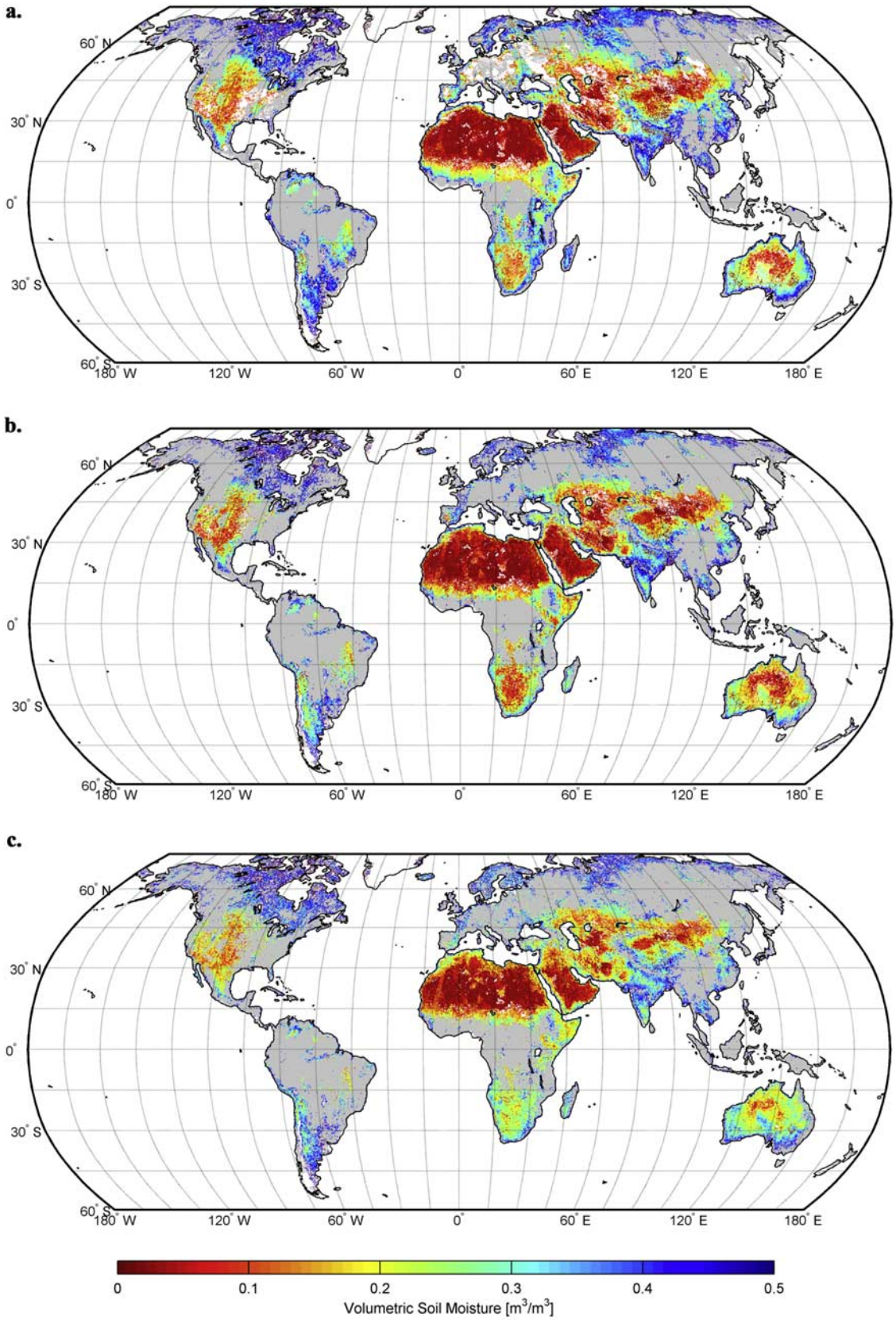

Figure 2. Monthly average Scanning Multichannel Microwave Radiometer surface soil moisture retrievals at (a) 6.6 GHz, (b) 10.7 GHz, and (c) 18 GHz for July 1980.

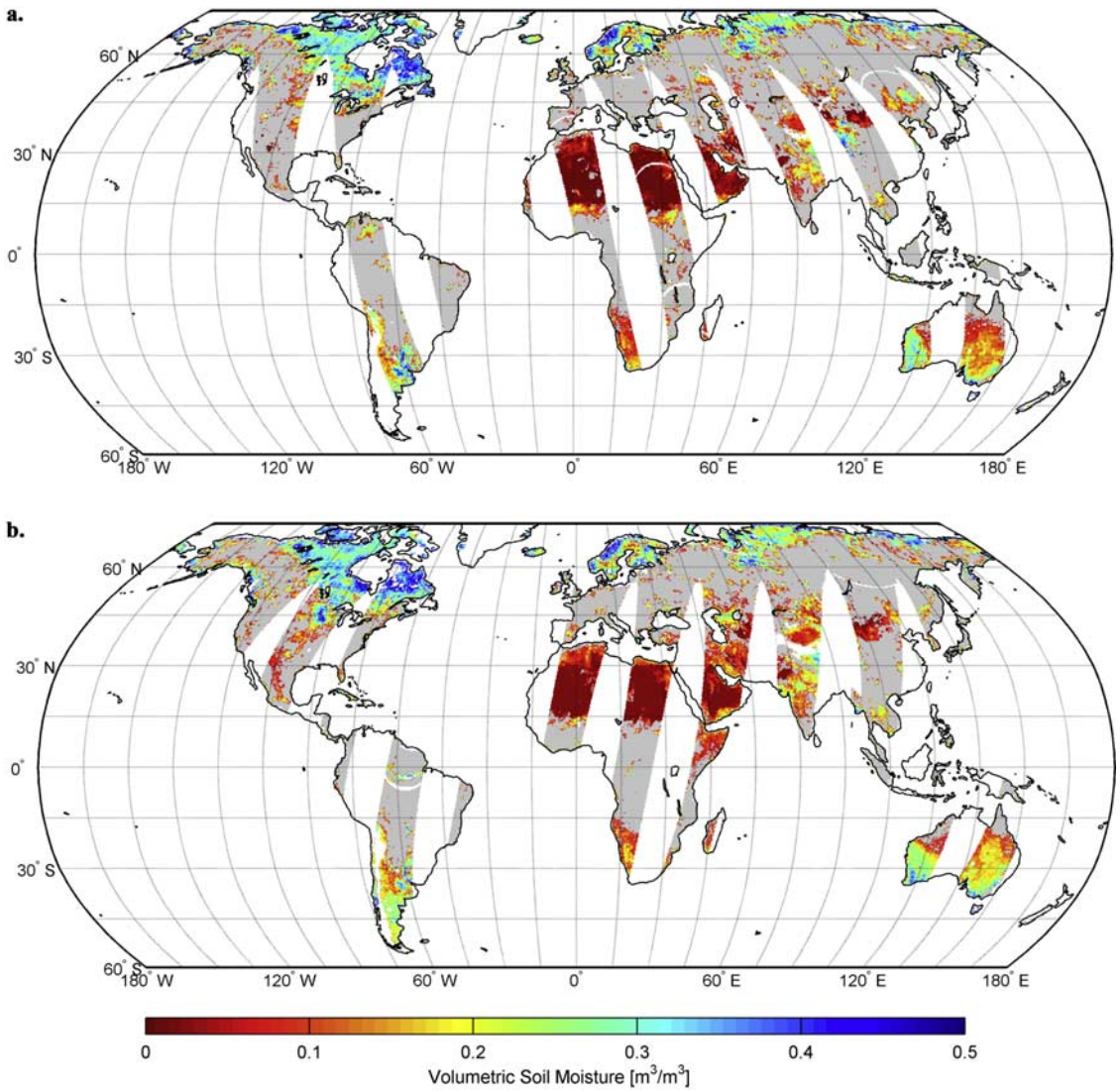

Figure 3. Twenty-four-hour day and night global Special Sensor Microwave Imager surface soil moisture retrievals for 7 July 2003.

2002. Even though TMI data are available beginning in 1997, global coverage does not extend beyond ±35° N and S. Therefore SSM/I will remain useful by providing soil moisture retrievals at those latitudes not covered by TMI. Daily SSM/I retrievals illustrate orbital coverage that is similar to SMMR, although swath widths of SSM/I are somewhat wider (Figure 3). Average monthly soil moisture retrievals also appear similar in their distribution, magnitude, and extent of coverage as previous SMMR retrievals at a similar waveband (Figure 4).

5.3. TRMM Microwave Imager

[37] The application of TMI soil moisture retrievals may potentially be somewhat more complex owing to the TRMM orbit characteristics. Since TMI is not a polar orbiter, the timing of daily coverage over any geographic location appears less systematic and almost random, although actually it is not. Daily coverage of polar orbiters occurs at the same local solar time at any given longitude, as the platform orbits the Earth. Furthermore, daytime and nighttime coverage for polar orbiters are typically archived separately, and are indicated as either ascending or descending orbits, respectively. However, TRMM is in a low-inclination orbit, extending from ±38° north and south, which does not lend itself well to such systematic separation. A series of selected daily orbit tracks (orbits 0, 2, and 4) is illustrated, and shows the timing and coverage characteristics of TMI throughout part of a 24-hour day (Figure 5). The resulting map of daily soil moisture retrievals is also illustrated (Figure 6). Patchiness in daily observations is frequently observed, and will result from soil moisture differences during subsequent overlapping and intersecting orbits as a result of precipitation events or extreme drying conditions.

5.4. Advanced Microwave Scanning Radiometer

[38] AMSR-E orbital coverage is similar to the other polar orbiting satellites, as illustrated in the daytime and nighttime surface soil moisture retrievals (Figure 7). The wider swath width, however, results in almost 100% daily

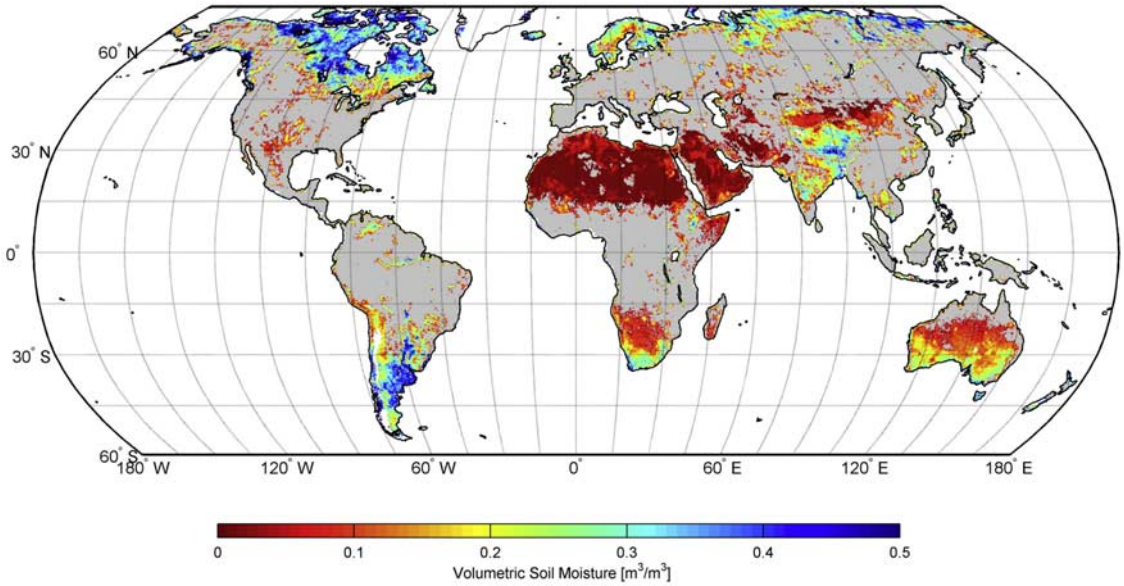

Figure 4. Monthly average global surface soil moisture for July 2003 as retrieved from Special Sensor Microwave Imager.

global coverage when the ascending and descending orbits are combined. One must keep in mind, however, that day and night coverage occurs at 12 hour intervals, and that the inherent timing information associated with the daytime and nighttime orbits would be lost during compositing. Average monthly global surface soil moisture retrievals for July 2003 are also illustrated for both 6.9 GHz and 10.7 GHz frequencies (Figure 8). From these two examples, it is observed that consistency between the two frequencies appears to be quite good. The presence of RFI is also seen to be greater in the C-band data, and is especially observed in the western and eastern portions of the U.S. These observations are also consistent with results found by *Li et al.* [2004].

6. Evaluation and Validation

[39] Surface soil moisture retrievals from earlier versions of the LPRM have been evaluated in several previous studies against both observational and model simulation data sets from a variety of global test sites, and compared quite well. These comparisons include test sites located in Illinois, Iowa, Mongolia, Russia, Turkmenistan (all from the Global Soil Moisture Data Bank), model simulation data

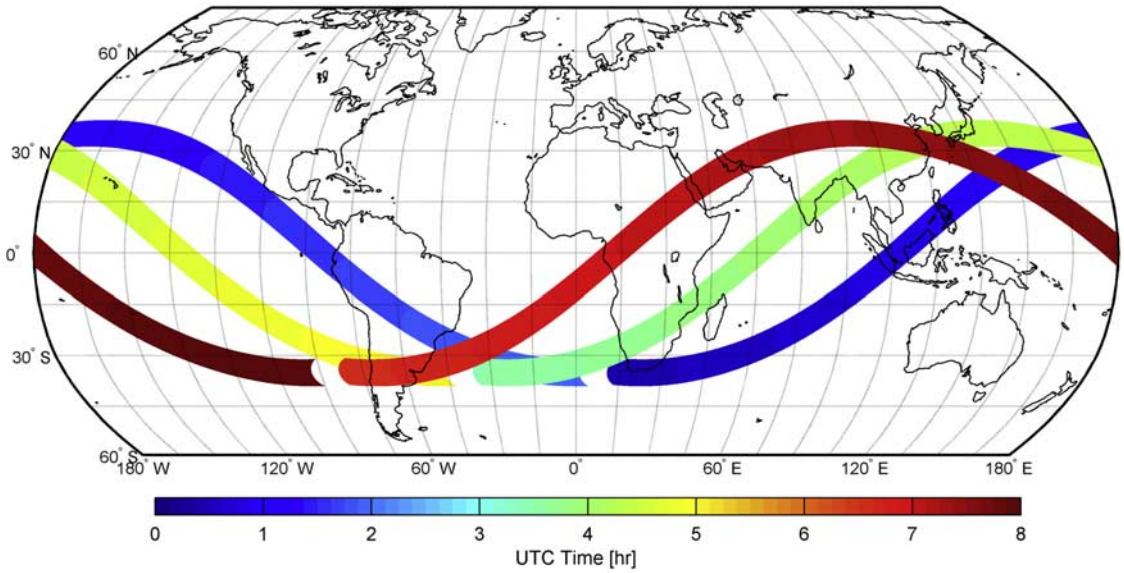

Figure 5. Selected Tropical Rainfall Measuring Mission orbit tracks during a 24-hour period, illustrating a typical pattern of daily coverage. A given daily pattern will repeat approximately every 47 days.

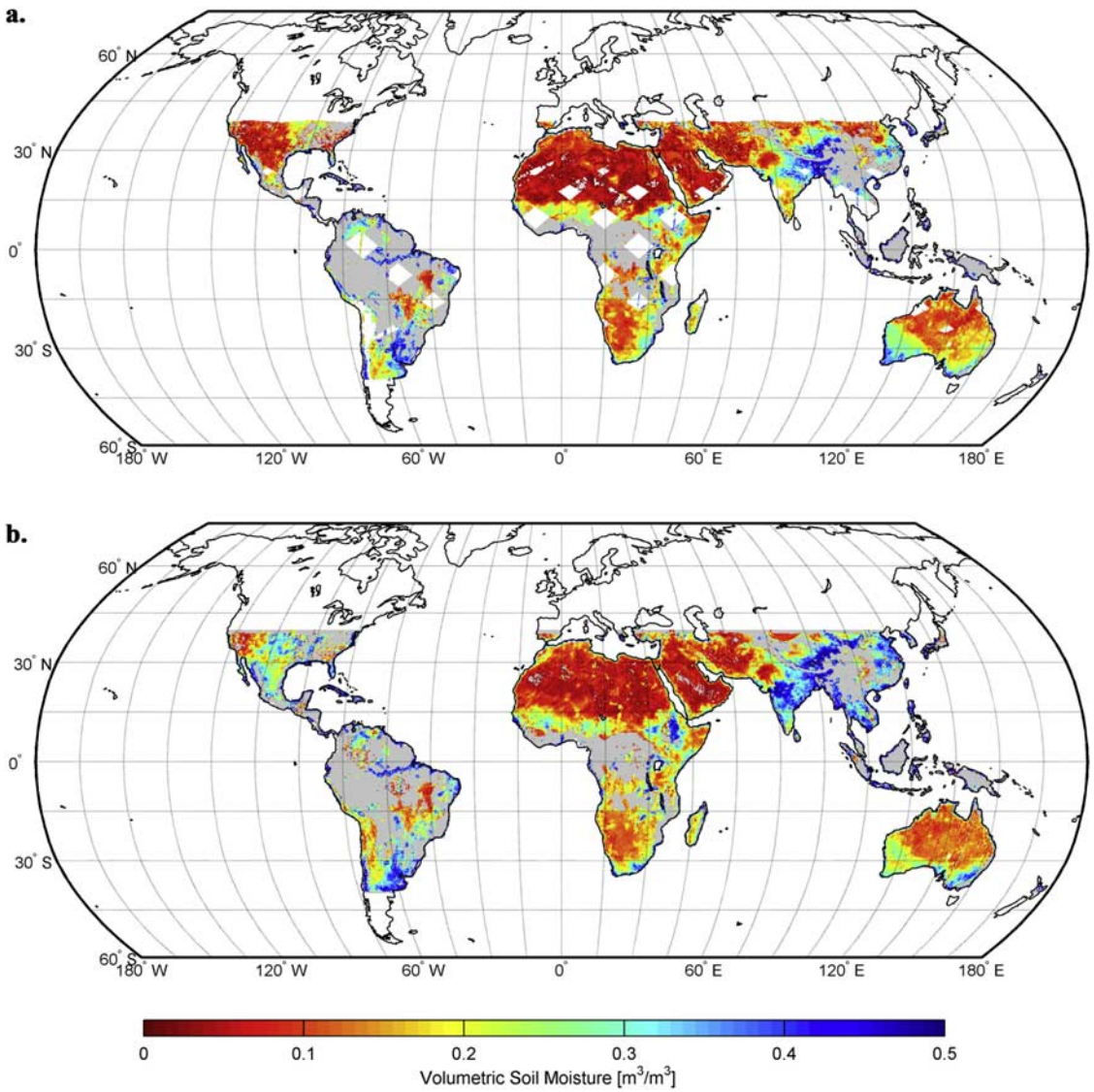

Figure 6. (a) Twenty-four-hour global surface soil moisture retrievals for 7 July and (b) average monthly global surface soil moisture retrievals for July 2003, derived from Tropical Rainfall Measuring Mission Microwave Imager at 10.7 GHz.

from the European Center for Medium-Range Weather Forecast (ECMWF) Model and the NASA Land Information System (LIS), and the Oklahoma Mesonet [*Owe et al.*, 2001; *De Jeu and Owe*, 2003; *O'Neill et al.*, 2006]. *Wagner et al.* [2007] compared surface soil moisture derived with 4 different satellite retrieval models with a dense network of surface soil moisture observations in central Spain, and found the LPRM to yield the highest correlation (R = 0.83) with the ground measurements.

[40] Additional validations in support of the new retrieval data sets are presented here. However, it is important to realize that very few observational data sets exist at the spatial and temporal scales and vertical sampling resolution necessary for optimal validation. The most widely used data sets are part of the Global Soil Moisture Data Bank, maintained at the Department of Environmental Sciences, Rutgers University [*Robock et al.*, 2000], and extensive comparisons have already been conducted with these data. While these data are among the best available, they are far from optimum, and several issues must be understood when using them for validating satellite-based retrievals. These include:

[41] 1. Differences in spatial resolution. Satellite data are spatial averages integrated over the entire footprint, whereas the ground data are point measurements and often with high spatial variability.

[42] 2. Differences in vertical resolution. The satellite data represent a soil sampling depth ranging from about 0.5 cm to 1.5 cm (depending on the sensor), whereas the ground measurements are often made at a depth of 10 cm or greater.

[43] 3. Differences in acquisition times. Satellite and ground observations rarely occur on the same day, and often as much as 5 to 7 days apart.

[44] 4. Interobservation periods. These periods may be as long as 10 days or more in some soil moisture data sets. It is

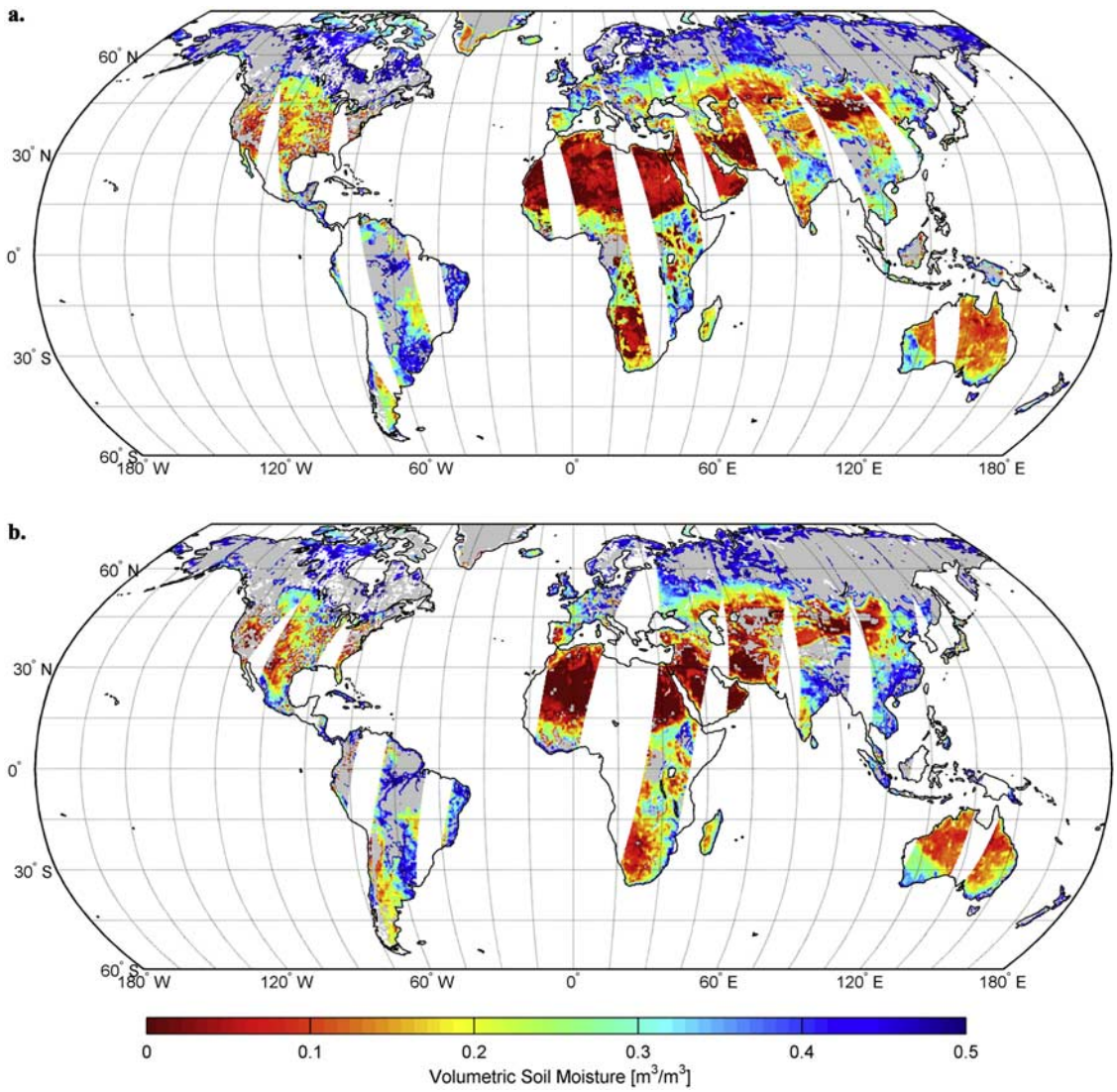

Figure 7. Twenty-four-hour global daytime and nighttime surface soil moisture retrievals for 7 July 2003 at 6.9 GHz from Aqua Advanced Microwave Scanning Radiometer for EOS.

important to realize that significant changes in surface moisture may occur during these interobservation periods that are often not captured by one or both of these data sets.

[45] An understanding these of issues is important when evaluating the validation process. The common expectation during validation is that two data sets agree as closely as possible. Unfortunately, this will often not be the case with the remote sensing data and ground observations, most notably for the reasons cited above. Because of this uncertainty, it is often more meaningful to compare time series trends than to make direct numerical comparisons.

[46] Time series of surface moisture retrievals from several satellite sensors are compared to averaged soil moisture observations from 7 measurement stations in southern Illinois [*Hollinger and Isard*, 1994]. The test site is approximately $1.5^\circ \times 2^\circ$ in size. Sampling was typically conducted 2 to 3 times per month by neutron probe, and reflects the average soil moisture in the top 10 cm. Please refer to the website, http://climate.envsci.rutgers.edu/soil_moisture/, for additional details pertaining to this data set. Land use/land cover descriptions for this test site are also provided in the work of *Owe et al.* [2001]. Surface moisture retrievals from SMMR (C band) for the period 1982–1987 are illustrated in Figures 9a and 9b. Retrieval data from AMSR-E (C band) are shown in Figure 9c, and exhibit similar patterns and magnitudes relative to the ground data as the SMMR data. This appears to indicate good consistency between the two instruments. The satellite retrievals are displayed as a 6-day mean trace of all footprint values falling within the test area during a daily orbit track. Six-day means were used in order to account for orbit tracks which may only have provided partial coverage of the test site on any given day and to make the satellite retrievals more readable. This approach is reasonable, especially in light of the coarse temporal resolution of the ground observations. The vertical dotted lines reflect the standard deviation of the individual retrieval values of all the footprints used to obtain a mean. Ground measurements are displayed as a mean trace with the full

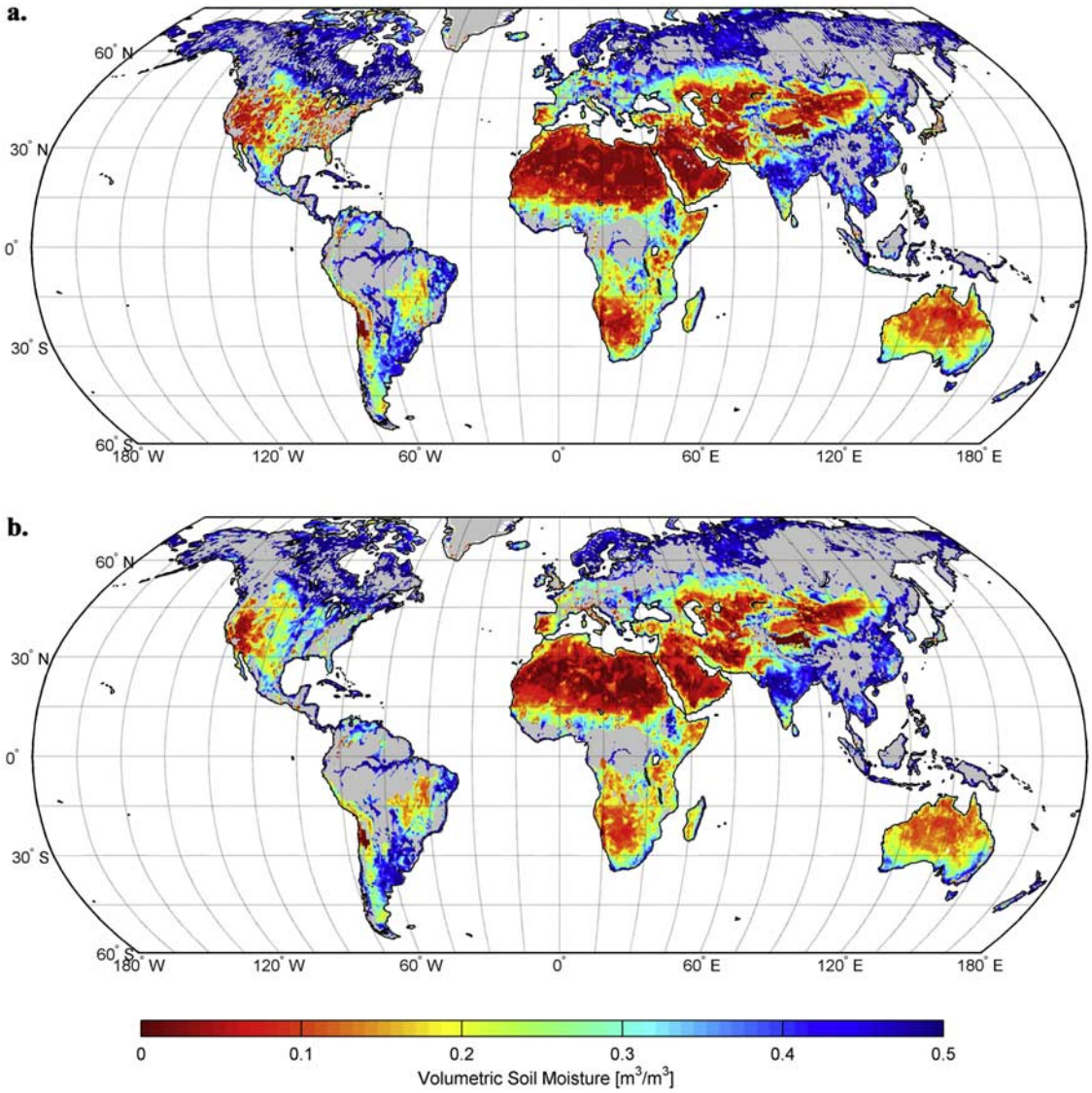

Figure 8. Average monthly global surface soil moisture retrievals at (a) 6.9 GHz and (b) 10.7 GHz from Aqua Advanced Microwave Scanning Radiometer for EOS for July 2003.

dynamic range indicated above and below. The spatial variability observed in both the satellite data and the ground data truly reflects the inherent nature of surface soil moisture. Satellite data coincide well with the ground data and tend to fall between the minimum and the mean ground data values for the most part, which is consistent with the fact that the sampling depth for the sensor is less than 1.5 cm. TRMM-TMI and AMSR-E X-band retrievals and SSM/I Ku-band data are illustrated in Figures 10 and 11, respectively. Again, the soil moisture data derived by these sensors are highly consistent with the ground data.

[47] A one-year daily time series of AMSR-E surface moisture retrievals is illustrated (Figure 12) for a 1° square test site in Oklahoma (35°–36° W and 98.5°–99.5° N), and compared to average daily soil moisture measurements from 8 observation stations from the Oklahoma Mesonet [*Brock et al.*, 1995]. Readers are referred to the website, http://www.mesonet.org/ for details concerning the Oklahoma Mesonet program, including site descriptions of the observation stations. Daily average surface moisture based on the satellite retrievals compare well to the site-averaged ground measurements taken at 5 cm. It is seen that the satellite observations are highly sensitive to changes in soil moisture at the surface, especially to rapid changes resulting from precipitation events. These changes are seen to be reflected in the deeper ground measurements as well, although not at the same magnitude and with some delay, since the soil in the top 1 cm surface layer will wet and dry much faster than at 5 cm.

7. Summary and Discussion

[48] A historical global soil moisture climatology is being developed from microwave radiometer measurements from multiple satellite sensors dating back to 1978. The surface moisture retrievals are derived with the Land Parameter

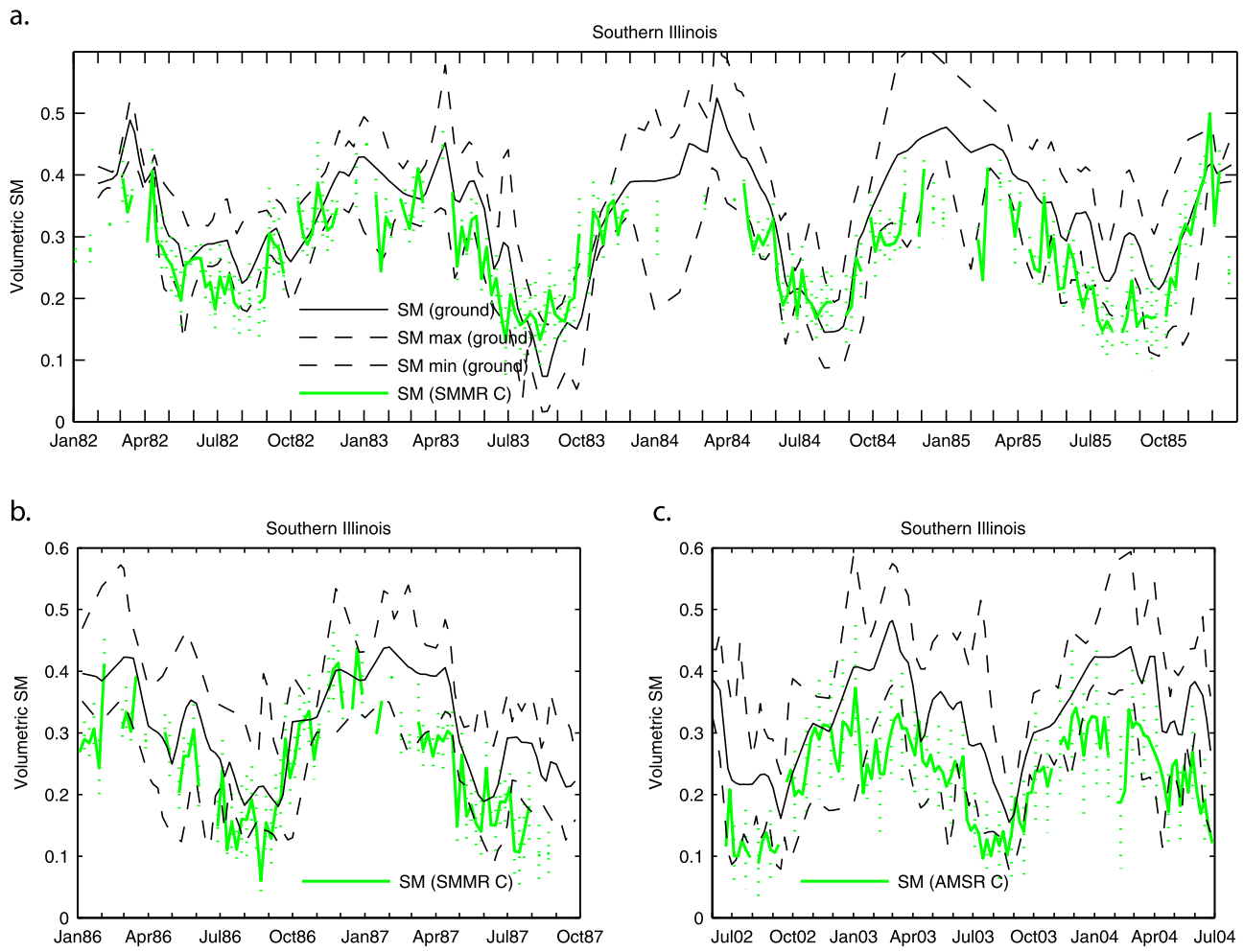

Figure 9. (a) Six-day average time series of Scanning Multichannel Microwave Radiometer (SMMR) 6.6-GHz surface moisture retrievals and ground measurements from 1982 through 1985 over southern Illinois. The dynamic range of the ground data and standard deviation of the satellite retrievals is also depicted. Also shown are the six-day average time series of (b) SMMR 6.6-GHz surface moisture retrievals (1986–1987) and (c) Aqua Advanced Microwave Scanning Radiometer for EOS 6.9-GHz retrievals (2002–2004) and corresponding ground measurements over southern Illinois.

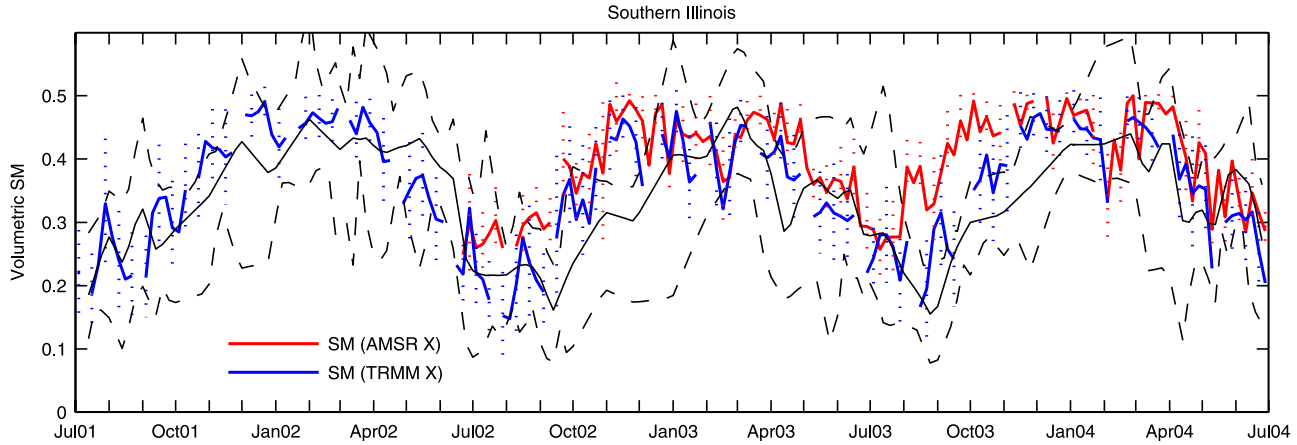

Figure 10. Six-day average time series of Aqua Advanced Microwave Scanning Radiometer for EOS 10.7-GHz and Tropical Rainfall Measuring Mission 10.7-GHz surface moisture retrievals and corresponding ground measurements in southern Illinois for the period 2001–2004.

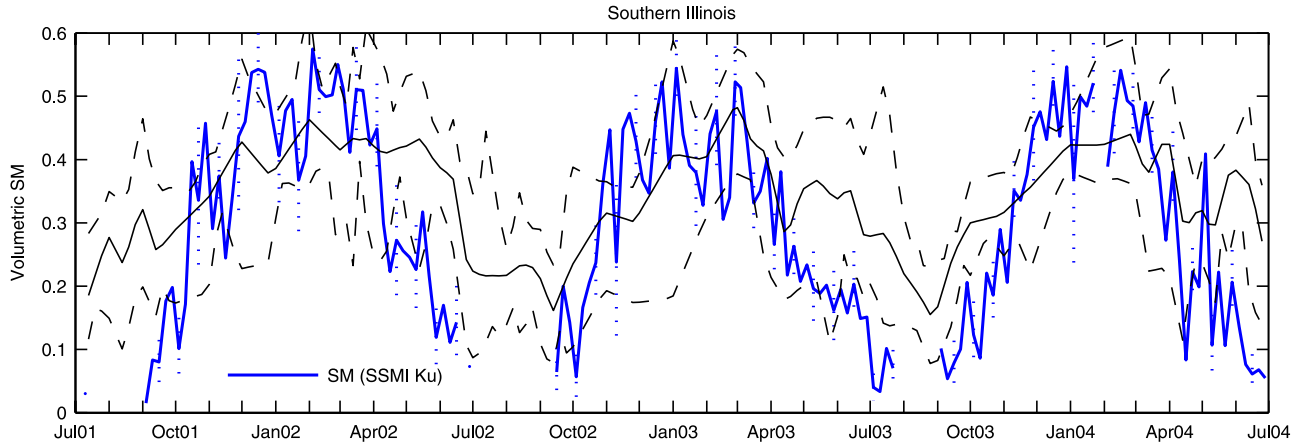

Figure 11. Six-day average time series of Special Sensor Microwave Imager 19.3-GHz surface moisture retrievals and corresponding ground data in southern Illinois for the period 2001–2004.

Retrieval Model. The data will be hosted at the Goddard Earth Sciences Data and Information Services Center (GES DISC), formerly known as the Goddard Distributed Active Archive Center (DAAC), and at the Vrije Universiteit Amsterdam, Netherlands, and will be made available for download by the scientific community. Data storage will be in HDF, which will maximize compatibility with other EOS era data sets. The sensors used in deriving surface soil moisture vary in frequency from C band to X band to K band, and users should understand the significance of wavelength differences in the interpretation of these data.

[49] Recommendations were made by several reviewers to include the dielectric constant as part of the data set. While this suggestion had not previously been considered, it could potentially add considerable value to the data set, such as in regions were the soil dielectric constant may be affected by high concentrations of salts, calcium, or other compounds. Efforts will be made to include this value-added data product.

[50] Examples of the global retrieval products from both historical and current sensors are presented and appear consistent with each other and with known global climatological zones. Additional data validation studies are also presented and evaluated together with observational soil moisture data sets. Comparisons between satellite and ground data appear quite good, considering the considerable differences in spatial coverage and the vertical sampling characteristics between the two data sets.

[51] Although a number of satellite-based soil moisture data products have been developed in recent years, most are limited in their spatial and temporal coverage or limited to only the AMSR-E period. The new data set is a global product, and is consistent in its retrieval approach for the entire period of data record. It must be remembered that the data retrievals are made from different sensors with somewhat different radiometric characteristics. This results in differences in thermal sensing depth, spatial resolution, acquisition times, and possibly other characteristics as well. While these data should prove useful for many types of environmental monitoring studies, users are encouraged exercise care in their interpretation, and especially in forming conclusions derived from long-term observational studies.

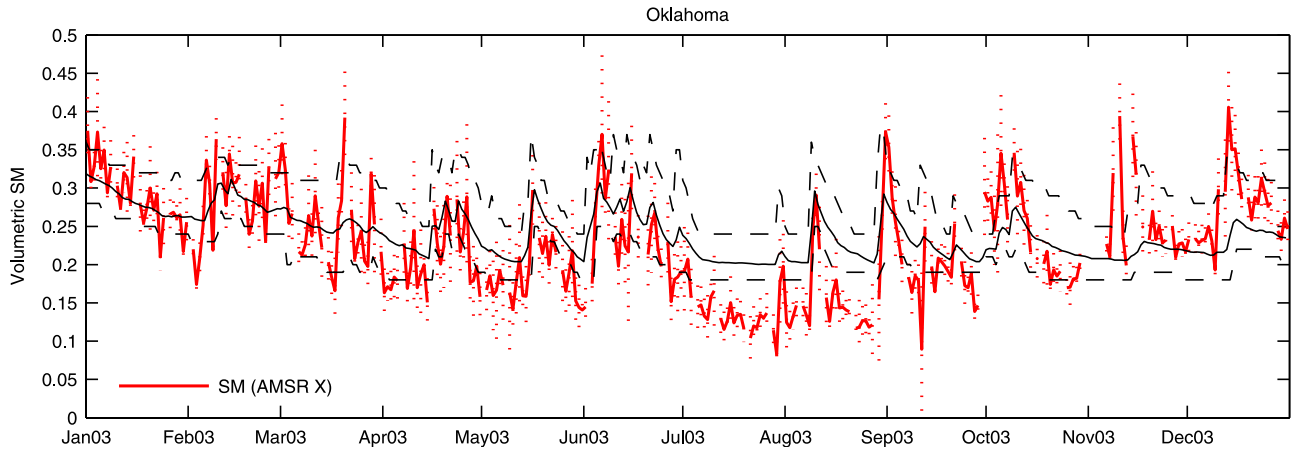

Figure 12. Time series of average daily Aqua Advanced Microwave Scanning Radiometer for EOS 6.9-GHz surface moisture retrievals and corresponding ground data for test site in western Oklahoma for 2003.

[52] **Acknowledgments.** Support for various phases of this research was provided by the Modeling, Analysis, and Prediction Branch of NASA Headquarters and the Department of Geo-environmental Sciences, Vrije Universiteit, Amsterdam. The authors would also like to thank the anonymous reviewers for their helpful recommendations.

References

Achutuni, R., and R. A. Schofield (1997), The spatial and temporal variability of the DMSP SSM/I global soil wetness index, paper presented at the 13th Conference on Hydrology, Am. Meteorol. Soc., Long Beach, Calif.

Ahmed, N. U. (1995), Estimating soil moisture from 6.6 GHz dual polarization, and/or satellite derived vegetation index, *Int. J. Remote Sens.*, *16*, 687–708.

Armstrong, R. L., K. W. Knowles, M. J. Brodzik, and M. A. Hardman (1994), *DMSP SSM/I Pathfinder Daily EASE-Grid Brightness Temperatures*, *June to September 2001*, [CD-ROM], Natl. Snow and Ice Data Cent., Boulder, Colo.

Ashcroft, P., and F. Wentz (2003), *AMSR-E/Aqua L2A Global Swath Spatially-Resampled Brightness Temperatures (Tb) V001*, *September to October 2003*, Natl. Snow and Ice Data Cent., Boulder, Colo.

Brock, F. V., K. C. Crawford, R. L. Elliott, G. W. Cuperus, S. J. Stadler, H. L. Johnson, and M. D. Eilts (1995), The Oklahoma Mesonet: A technical overview, *J. Atmos. Oceanic Technol.*, *12*, 5–19.

Choudhury, B. J., T. J. Schmugge, A. T. C. Chang, and R. W. Newton (1979), Effect of surface roughness on the microwave emission from soils, *J. Geophys. Res.*, *84*, 5699–5705.

De Jeu, R. A. M., and M. Owe (2003), Further validation of a new methodology for surface moisture and vegetation optical depth, *Int. J. Remote Sens.*, *24*, 4559–4578.

Dobson, M. C., F. T. Ulaby, M. T. Hallikainen, and M. A. El-Rayes (1985), Microwave dielectric behavior of wet soil—part II: Dielectric mixing models, *IEEE Trans. Geosci. Remote Sens.*, *23*, 35–46.

Drusch, M., E. F. Wood, and T. J. Jackson (2001), Vegetative and atmospheric corrections for the soil moisture retrieval from passive microwave remote sensing data: Results from the Sothern Great Plains Hydrology Experiment 1997, *J. Hydrometeorol.*, *2*, 181–192.

Gloersen, P., and F. T. Barath (1977), A scanning multichannel microwave radiometer for Nimbus-G and SeaSat-A, *IEEE J. Oceanic Eng.*, *2*, 172–178.

Gloersen, P., et al. (1984), A summary of results from the first Nimbus-7 observations, *J. Geophys. Res.*, *89*, 5335–5344.

Hollinger, S. E., and S. A. Isard (1994), A soil moisture climatology of Illinois, *J. Clim.*, *7*, 822–833.

Jackson, T. J. (1993), Measuring surface soil moisture using passive microwave remote sensing, *Hydrol. Processes*, *7*, 139–152.

Jackson, T. J. (1997), Soil moisture estimation using special sensor microwave/imager satellite data over a grassland region, *Water Resour. Res.*, *18*, 1475–1484.

Jackson, T. J., and A. Y. Hsu (2001), Soil moisture and TRMM microwave imager relationships in the Southern Great Plains 1999 (SGP99) Experiment, *IEEE Trans. Geosci. Remote Sens.*, *39*, 1632–1642.

Jackson, T. J., and P. E. O'Neill (1987), Salinity effects on the microwave emission of soils, *IEEE Trans. Geosci. Remote Sens.*, *GE-25*, 214–220.

Jackson, T. J., and T. J. Schmugge (1991), Vegetation effects on the microwave emission from soils, *Remote Sens. Environ.*, *36*, 203–212.

Jackson, T. J., T. J. Schmugge, and J. R. Wang (1982), Passive microwave sensing of soil moisture under vegetation canopies, *Water Resour. Res.*, *18*, 1137–1142.

Jackson, T. J., T. J. Schmugge, and P. E. O'Neill (1984), Passive microwave remote sensing of soil moisture from an aircraft platform, *Remote Sens. Environ.*, *14*, 135–152.

Jackson, T. J., K. G. Kostov, and S. S. Saatchi (1992), Rock fraction effects on the interpretation of microwave emission from soil, *IEEE Trans. Geosci. Remote Sens.*, *30*, 610–616.

Jackson, T. J., D. M. Le Vine, C. T. Swift, T. J. Schmugge, and F. R. Schiebe (1995), Large area mapping of soil moisture using the ESTAR passive microwave radiometer in Washita '92, *Remote Sens. Environ.*, *53*, 27–37.

Jackson, T. J., P. E. O'Neill, and C. T. Swift (1997), Passive microwave observation of diurnal surface soil moisture, *IEEE Trans. Geosci. Remote Sens.*, *35*, 184–194.

Jackson, T. J., D. M. Le Vine, A. Y. Hsu, A. Oldak, P. J. Starks, C. T. Swift, J. D. Isham, and M. Haken (1999), Soil moisture mapping at regional scales using microwave radiometry: The Southern Great Plains Hydrology Experiment, *IEEE Trans. Geosci. Remote Sens.*, *37*, 2136–2151.

Jackson, T. J., A. Y. Hsu, and P. E. O'Neill (2002), Surface soil moisture retrieval and mapping using high frequency microwave satellite observations in the southern great plains, *J. Hydrometeorol.*, *3*, 688–699.

Kirdiashev, K. P., A. A. Chukhlantsev, and A. M. Shutko (1979), Microwave radiation of the Earth's surface in the presence of vegetation cover, *Radio Eng. Electron.*, *24*, 256–264.

Kummerow, C., W. Barnes, T. Kozu, J. Shiue, and J. Simpson (1998), The Tropical Rainfall Measuring Mission (TRMM) sensor package, *J. Atmos. Oceanic Technol.*, *15*, 809–817.

Li, L., E. G. Njoku, E. Im, P. S. Chang, and K. St. Germaine (2004), A preliminary survey of radio-frequency interference over the U.S. in Aqua AMSR–E data, *IEEE Trans. Geosci. Remote Sens.*, *42*, 380–390.

McFarland, M. J. (1976), The correlation of Skylab L-band brightness temperatures with antecedent precipitation, paper presented at 1st Conference on Hydrometeorology, Am. Meteorol. Soc., Boston, Mass.

McFarland, M. J., and C. M. U. Neale (1991), Land parameter algorithm validation and calibration, in *DMSP Special Sensor Microwave/Imager Calibration/Validation*, *Final Rep.*, vol. II, edited by J. P. Hollinger, pp. 9-1–9-108, Naval Res. Lab., Washington, D. C.

Meesters, A. G. C. A., R. A. M. de Jeu, and M. Owe (2005), Analytical derivation of the vegetation optical depth from the microwave polarization difference index, *IEEE Trans. Geosci., Remote Sens.*, *2*, 121–123.

Mo, T., B. J. Choudhury, T. J. Schmugge, J. R. Wang, and T. J. Jackson (1982), A model for microwave emission from vegetation-covered fields, *J. Geophys. Res.*, *87*, 11,229–11,237.

National Research Council (1990), Research strategies for the U.S. Global Change Research Program, 292 pp., Comm. on Global Change, Comm. on Geosci., Environ., and Resour., Natl. Acad. of Sci., Natl. Acad. Press, Washington, D. C.

National Research Council (2007), Earth science and applications from space: National imperatives for the next decade and beyond, Committee on Earth Science and Applications from Space: A Community Assessment and Strategy for the Future, 437 pp., Space Stud. Board, Div. of Eng. and Phys. Sci., Natl. Acad. of Sci., Natl. Acad. Press, Washington, D. C.

National Snow and Ice Data Center (NSIDC) (2005a), Nimbus-7 SMMR pathfinder daily EASE-grid brightness temperatures, Boulder, Colo.

National Snow and Ice Data Center (NSIDC) (2005b), DMSP SSM/I pathfinder daily EASE-grid brightness temperatures, Boulder, Colo.

National Snow and Ice Data Center (NSIDC) (2006), Data products and services, Boulder, Colo.

Njoku, E. (2004), AMSR-E/Aqua Daily L3 Surface Soil Moisture, V001, Natl. Snow and Ice Data Cent., Boulder, Colo.

Njoku, E., and L. Li (1999), Retrieval of land surface parameters using passive microwave measurements at 6–18 GHz, *IEEE Trans. Geosci. Remote Sens.*, *37*, 79–93.

Njoku, E., T. Jackson, V. Lakshmi, T. Chan, and S. V. Nghiem (2003), Soil moisture retrieval from AMSR-E, *IEEE Trans. Geosci. Remote Sens.*, *41*, 215–229.

Njoku, E., P. Ashcroft, T. K. Chan, and L. Li (2005), Statistics and global survey of radio-frequency interference in AMSR-E land observations, *IEEE Trans. Geosci. Remote Sens.*, *43*, 938–947.

O'Neill, P. E., and T. J. Jackson (1990), Observed effects of soil organic matter content on the microwave emissivity of soils, *Remote Sens. Environ.*, *31*, 175–182.

O'Neill, P. E., E. G. Njoku, J. Shi, E. F. Wood, M. Owe, and B. Gouweleeuw (2006), Hydros soil moisture retrieval algorithms: Status and relevance to future missions, paper presented at IEEE International Geoscience and Remote Sensing Symposium 2006 (IGARSS 2006), Denver, Colo., 31 July to 4 Aug.

Owe, M., and A. A. Van de Griend (2001), On the relationship between thermodynamic surface temperature and high frequency (37 GHz) vertical polarization brightness temperature under semi-arid conditions, *Int. J. Remote Sens.*, *22*, 3521–3532.

Owe, M., A. T. C. Chang, and R. E. Golus (1988), Estimating surface soil moisture from satellite microwave measurements and a satellite-derived vegetation index, *Remote Sens. Environ.*, *24*, 33l–345.

Owe, M., A. A. Van de Griend, and A. T. C. Chang (1992), Surface moisture and satellite microwave observations in semiarid southern Africa, *Water Resour. Res.*, *28*, 829–839.

Owe, M., R. A. M. de Jeu, and J. Walker (2001), A methodology for surface soil moisture and vegetation optical depth retrieval using the microwave polarization difference index, *IEEE Trans. Geosci. Remote Sens.*, *39*, 1643–1694.

Owe, M., T. Holmes, De R. Jeu (2005), A physically based model with remote sensing inputs for improved soil temperature retrievals, paper presented at 1st International Symposium on Remote Sensing of Environment, Int. Soc. for Optical Eng., St. Petersburg, Russia, 20–24 June.

Rees, W. G. (2001), *Physical Principles of Remote Sensing*, 372 pp., Cambridge Univ. Press, New York.

Robock, A., K. Y. Vinnikov, G. Srinivasan, J. K. Entin, S. E. Hollinger, N. A. Speranskaya, S. Liu, and A. Namkhai (2000), The global soil moisture data bank, *Bull. Am. Meteorol. Soc.*, *81*, 1281–1299.

Rodell, M., et al. (2004), The global land data assimilation system, *Bull. Am. Meteorol. Soc.*, *85*, 381–394.

Schmugge, T. J. (1976), Remote sensing of soil moisture, *Doc. X-913-76-118*, 21 pp., NASA Goddard Space Flight Cent., Greenbelt, Md.

Schmugge, T. J. (1977), Remote sensing of surface soil moisture, *J. Appl. Meteorol.*, *17*, 1549–1557.

Schmugge, T. J. (1983), Remote sensing of soil moisture: Recent advances, *IEEE Trans. Geosci. Remote Sens.*, *21*, 336–344.

Schmugge, T. J. (1985), Remote sensing of soil moisture, in *Hydrological Forecasting*, edited by M. G. Anderson and T. P. Burt, pp. 101–124, John Wiley, Hoboken, N. J.

Van de Griend, A. A., and M. Owe (1994), Microwave vegetation optical depth and inverse modelling of soil emissivity using Nimbus/SMMR satellite observations, *Meteorol. Atmos. Phys.*, *54*, 225–239.

Wagner, W., V. Naeimi, K. Scipal, R. de Jeu, and J. Martinez-Fernanadez (2007), Soil moisture from operational meteorological satellites, *Hydrogeol. J.*, *15*, 121–131.

Wang, J. R., and B. J. Choudhury (1981), Remote sensing of soil moisture content over bare field at 1.4 GHz frequency, *J. Geophys. Res.*, *86*, 5277–5282.

Wang, J. R., and T. J. Schmugge (1980), An empirical model for the complex dielectric permittivity of soil as a function of water content, *IEEE Trans. Geosci. Remote Sens.*, *18*, 288–295.

Wegmuller, U., C. Maetzler, and E. G. Njoku (1995), Canopy opacity models, in *Passive Microwave Remote Sensing of Land-Atmosphere Interactions*, edited by B. J. Choudhury et al., pp. 375–387, VSP Int. Sci. Publ., Utrecht, Netherlands.

Wigneron, J. P., A. Chanzy, J. C. Calvet, and N. Bruguier (1995), A simple algorithm to retrieve soil moisture and vegetation biomass using passive microwave measurements over crop fields, *Remote Sens. Environ.*, *51*, 331–341.

Wilke, G. D., and M. J. McFarland (1986), Correlations between Nimbus 7 scanning multichannel microwave radiometer (SMMR) data and an antecedent precipitation index, *J. Clim. Appl. Meteorol.*, *25*, 227–238.

R. de Jeu and T. Holmes, Department of Geo-Environmental Sciences, Vrije Universiteit Amsterdam, De Boelelaan 1085, NL-1081 HV Amsterdam, Netherlands.

M. Owe, Hydrological Sciences Branch, NASA Goddard Space Flight Center, Mail Code 614.3, Greenbelt, MD 20771, USA. (manfred.owe@nasa.gov)